

# Nonlinear numerical modelling for the effects of surface explosions on buried reinforced concrete structures

N. Nagy<sup>1</sup>, M. Mohamed<sup>2\*</sup> and J.C. Boot<sup>2</sup>

<sup>1</sup>*MTC, Egypt*

<sup>2</sup>*School of Engineering, Design and Technology, University of Bradford, Bradford, West Yorkshire, BD7 1DP, UK*

*(Received September 18, 2009, Accepted January 26, 2010)*

**Abstract.** The analysis of structure response and design of buried structures subjected to dynamic destructive loads have been receiving increasing interest due to recent severe damage caused by strong earthquakes and terrorist attacks. For a comprehensive design of buried structures subjected to blast loads to be conducted, the whole system behaviour including simulation of the explosion, propagation of shock waves through the soil medium, the interaction of the soil with the buried structure and the structure response needs to be simulated in a single model. Such a model will enable more realistic simulation of the fundamental physical behaviour. This paper presents a complete model simulating the whole system using the finite element package ABAQUS/Explicit. The Arbitrary Lagrange Euler Coupling formulation is used to model the explosive charge and the soil region near the explosion to eliminate the distortion of the mesh under high deformation, while the conventional finite element method is used to model the rest of the system. The elasto-plastic Drucker-Prager Cap model is used to model the soil behaviour. The explosion process is simulated using the Jones-Wilkens-Lee equation of state. The Concrete Damage Plasticity model is used to simulate the behaviour of concrete with the reinforcement considered as an elasto-plastic material. The contact interface between soil and structure is simulated using the general Mohr-Coulomb friction concept, which allows for sliding, separation and rebound between the buried structure surface and the surrounding soil. The behaviour of the whole system is evaluated using a numerical example which shows that the proposed model is capable of producing a realistic simulation of the physical system behaviour in a smooth numerical process.

**Keywords:** soil-structure interaction; numerical modelling; surface explosion; buried structure.

---

## 1. Introduction

Investigating the response of buried structures under the effect of blast loads is of interest in many fields of engineering such as structural engineering, geotechnical engineering, and mining engineering. Buried structures such as shelters, military protective structures and tunnels are essential during for example a military crisis to grant continuity of government, to provide military command centres and to protect the general public.

Currently, the effects of different kinds of explosion on buried structures are undertaken using

---

\*Corresponding author, Ph.D., E-mail: [m.h.a.mohamed@bradford.ac.uk](mailto:m.h.a.mohamed@bradford.ac.uk)

empirical or semi-empirical methods that were developed based on field tests (TM 5-855-1 1986). In this case, the free-field stresses are calculated at the expected structure location. These stresses are then modified to approximate the effects of the structure and its response. Then these modified interface stresses are applied on the structure. It should be noted that the response of the buried structure cannot be accurately predicted unless the loads on the structure are measured accurately. This can be achieved if a finite element model of the explosion-soil-structure system is developed without decoupling the free-field analysis from the structure response analysis. Recently different types of numerical methods have been used to investigate the response of buried reinforced concrete structures under blast loads. They can be classified as either uncoupled or coupled systems.

In the uncoupled system, the main physical procedure is divided into several successive stages; the results of each stage are the input of the following stage. Accordingly, the solution can be achieved in three stages which are (i) the explosion process and the formation of crater or cavity; (ii) the blast wave propagation; and (iii) the response of the structure itself. Many numerical investigations were conducted using the uncoupled system (see for example, TM 5-855-1 1986, Yang 1997, Hinman 1989a). In the uncoupled system, the free field stress histories are measured first and then these time histories are applied on the structure as boundary conditions for evaluating the structure response. Therefore, the interaction between the soil and the structure cannot be considered in a truly realistic way.

Coupled procedures can be divided into two categories:

- i. In the incomplete coupled method, the above mentioned three stages are reduced to two, with either the first two or the last two stages being fused.
- ii. Conversely, the complete coupled method unites all the three stages together in only one model (Stevens *et al.* 1991, Wang *et al.* 2005, Lu *et al.* 2005).

So far numerical complete coupled methods without assumptions in any part of the model have never been presented in the open technical literature. However, several numerical investigations were conducted to analyse the response of buried structures under explosion effects using an uncoupled system or the incomplete coupled method (Stevens and Krauthammer 1988, Hinman 1989b, Baylot 1992, Zhang *et al.* 2002, Kanarachos and Provatidis 1998, O'Daniel and Krauthammer 1997, Weidlinger and Hinman 1988).

An approach has been developed combining the finite difference technique (FDT) with the finite element method (FEM) (Zimmerman *et al.* 1990a and b). In this approach the soil was modelled by FDT which is suitable for analyzing wave propagation in a continuous nonlinear medium, while the structure was modelled by the FEM. These coupled approaches considered the dynamic soil structure interaction and the coupling effect between the soil and structure, but the blast loading was still defined in terms of stress or pressure time histories. While it may be considered appropriate to define the blast loading as a pressure loading for relatively simple and symmetric situations, it becomes problematic in cases of irregular shape of the structure or when the ground surface effect becomes significant as in the case of shallow buried structures (Yang 1997). In these situations, a fully coupled approach including the explosion source is needed.

In general the interaction effects such as slippage, separation, and rebound, are significant aspects of the overall problem that affect the structure response. To take these into account, several coupled analysis techniques emerged. It is stated that the interaction between the shock wave and the structure, particularly for a structure with complex geometry, the ground reflection, as well as the blast-induced ground vibration effect, are difficult to simulate in a realistic manner with an uncoupled

model (Lu and Wang 2006). The coupling effect is significant, particularly when the structure is in a dense medium such as soil or water (Henrych 1979). To take these effects into account, complete coupled analysis techniques without artificial assumptions should be used.

Most studies based on either the uncoupled system or the incomplete coupled method do not consistently define either the loads on the structure or the interaction between the structure and the surrounding soil. Some studies approximate either soil, structure or both as elastic materials (Yang 1997). Whilst others do not allow for arbitrary soil-structure interaction effects by merging the interface nodes between the soil and the structure (Chen *et al.* 1990).

Very recently some numerical investigations have been reported which feature a complete coupled numerical analysis of the desired problem using a combination of Smooth Particle Hydrodynamics (SPH) and the conventional FEM, but with some assumptions made concerning the interaction between the structure and the surrounding soil (Wang *et al.* 2005, Lu *et al.* 2005). In this analysis the SPH method is used only to model the near field medium to the explosive charge to present the crater formation and to overcome the numerical problems resulting from the large deformation as the soil in the vicinity of the charge experiences large deformations. While the conventional FEM is used to model the intermediate and the far field soil medium and the structural response. The interface between the buried concrete structure and the surrounding soil is modelled using a fully consistent FEM mesh for the structure with the nodes of the soil mesh fused to the nodes of the structure mesh at the interface. The interface modelling was undertaken in this manner based on the experimental results of Mueller (1986). Of note, Mueller (1986) investigated experimentally the interface characteristics between sand and rough grout. It was found that the yield points of the interface clustered close to the sand yield line. The results of Mueller (1986) also suggested that the failure mainly occur within the sand and not at the interface. In other words, the characteristics of the interface are controlled by the properties of sand rather than by the contact's properties. Wang *et al.* (2004) developed a soil model that accounts for friction, bond between the solid particles and the damage that might occur to the soil skeleton. Utilising the new soil model and modelling the interface as completely joined surfaces will limit the failure to occur in the soil rather than at the interface. This approach would be acceptable for rough interfaces. However, as suggested and recommended by previous researchers (Hinman 1989, Weidlinger and Hinman 1988, Yang 1997) that to enhance the predictions, consistent modelling of the interface conditions must allow for sliding, separation, and rebound by applying a friction coefficient between the two surfaces.

Due to all these simplifying numerical assumptions, the existing simulations are some way from replicating the realistic behaviour of the system. This highlights that there is a need to simulate the response of buried structures subjected to blast loads with a complete coupled model without any artificial assumptions. The complete coupled analysis model should be able to simulate the explosion of the charge, the propagation of stresses through the soil, the interaction of the structure with the surrounding soil and the structure response in one single stage. In particular the cost of providing any experimental test data on buried structure response to explosions continues to prevent any such data appearing in the open literature (in addition to security and confidentiality issues, especially with respect to military applications). The development of a reliable complete numerical analysis will therefore be a significant step forward for the designers of these installations.

In this paper a complete coupled model is proposed employing nonlinear material models to represent the realistic behaviour of the different physical elements of the problem. The Arbitrary Lagrange Euler Coupling formulation (ALE) is used in the explosion and soil region near the explosion to eliminate the distortion of the mesh under high deformation (Hu and Randolph 1998).

Whereas, the conventional Finite Element Method (FEM) is utilised to model the rest of the system. The elasto-plastic Drucker-Prager Cap model is used to simulate the soil behaviour. The Concrete Damage Plasticity model is used to simulate the behaviour of concrete with the reinforcement taken to be an elasto-plastic material. The explosion process is simulated using the respected Jones-Wilkens-Lee (JWL) equation of state. The contact interface between the soil and the structure is simulated using the general Mohr-Coulomb friction concept, which allows for sliding, separation, and rebound between the buried structure surface and the surrounding soil. The behaviour of the whole system is evaluated using a numerical example.

## 2. Modelling techniques

For accurate investigations of the effects of blast loads on buried structures, nonlinear material models are applied. A summary description of the material models assigned for the explosive charge, soil mass, reinforced concrete structure and interaction between soil and structure is presented in this section.

### 2.1 Soil model

Since there is no time for drainage to occur under impact/blast loading, the soil mass can be considered as a single phase material under these conditions, and a total stress analysis can be carried out (MIL-HDBK-1007/3 1997 and Helwany 2007). In this investigation the clayey soil is considered and its behaviour is simulated by an elasto-plastic Drucker-Prager Cap model. This was originally developed to predict the plastic deformation of soils under compression (Drucker and Prager 1952, Chen and Mizuno 1990). It consists principally of two intersecting segments: a shear failure segment  $F_s$  and a cap segment  $F_c$  which provides an inelastic hardening mechanism to account for plastic compaction and helps to control volume dilatancy when the material yields in shear. A transition segment  $F_t$  has been introduced to provide a smooth surface between the shear failure surface and cap segment. Full details of this model, including definition and derivation of all necessary parameters are available in Chen and Mizuno (1990). Typical model parameters used for the clay soil are shown in Table 1.

### 2.2 Explosive charge model

The charge is modelled using the JWL equation of state. It simulates the pressure ( $P$ ) generated by expansion of the detonation product or the chemical energy of a chemical explosive (Lee *et al.* 1968, Lee *et al.* 1973). This model has been widely used in engineering applications. The JWL equation of state can be written in terms of the initial energy per unit mass,  $E_{m0}$  as follows

$$P = A \left( 1 - \frac{\omega \rho}{R_1 \rho_0} \right) \exp \left( -R_1 \frac{\rho}{\rho_0} \right) + B \left( 1 - \frac{\omega \rho}{R_2 \rho_0} \right) \exp \left( -R_2 \frac{\rho}{\rho_0} \right) + \frac{\omega \rho^2}{\rho_0} E_{m0} \quad (1)$$

where  $A$ ,  $B$ ,  $R_1$ ,  $R_2$  and  $\omega$  are material constants which for many common explosives have been determined from dynamic experiments.  $\rho_0$  is the density of the explosive and  $\rho$  is the density of the detonation products. The initial relative density ( $\rho/\rho_0$ ) used in the JWL equation is assumed to

Table 1 Material properties of the clay soil

Parameters	Soil
Young's modulus ( $E$ )	51.7 MPa
Poisson's ratio ( $\nu$ )	0.45
Density ( $\rho$ )	1920 kg/m <sup>3</sup>
Material cohesion ( $d$ )	0.036 MPa
Material angle of friction ( $\beta$ )	24°
Cap eccentricity parameter ( $R$ )	0.3
Initial cap yield surface position ( $\epsilon_v$ )	0.02
Transition surface radius parameter ( $\alpha$ )	0.0
Cap hardening behaviour ( <i>Stress, plastic volumetric strain</i> )	2.75 MPa, 0.00 4.83 MPa, 0.02 5.15 MPa, 0.04 6.20 MPa, 0.08

Table 2 JWL parameters used for modelling TNT explosive

Parameters	Value
Detonation wave speed, $C_d$	6930 m/s
A	373.8 GPa
B	3.747 GPa
$R_1$	4.15
$R_2$	0.9
$\omega$	0.35
The density of the explosive, $\rho_0$	1630 Kg/m <sup>3</sup>
Initial specific energy $E_{m0}$	3.63 Joule/kg

be unity, therefore nonzero values of initial specific energy  $E_{m0}$  should be specified. In the analyses the TNT explosive charges have been modelled by the JWL equation of state with properties as presented by Wang *et al.* (2004). The parameters for the TNT charge are listed in Table 2.

### 2.3 Reinforced concrete structure model

To best simulate the behaviour of a reinforced concrete structure, the concrete and steel are modelled independently as follows:

#### 2.3.1 Concrete model

The mechanical behaviour of concrete is modelled using the Concrete Damage Plasticity (CDP) constitutive model. The CDP model uses the concepts of isotropic damaged elasticity in combination with isotropic tensile and compressive plasticity to represent the inelastic behaviour of concrete. The CDP model provides a general capability for modelling plain or reinforced concrete in applications involving dynamic loading. This model can be used to simulate the irreversible damage involved in the fracturing process and the recovery of stiffness as loads change from tension to compression or vice versa. The constitutive theory for this model aims to capture the effects of irreversible damage

Table 3 Material properties of the concrete structure

The parameters of CDP model		Value	
<i>Young's modulus E</i> (GPa)		19.7	
Poisson's ratio $\nu$		0.19	
$\beta$		38 <sup>0</sup>	
Flow potential eccentricity ( $\varepsilon$ )		1	
$\sigma_{b0}/\sigma_{c0}$		1.12	
$K_c$		0.666	
Concrete compression hardening		Concrete compression damage	
Stress [Pa]	Crushing strain	Damage	Crushing strain
15.0e6	0.0	0.0	0.0
20.197804e6	0.0000747307	0.0	0.0000747307
30.000609e6	0.0000988479	0.0	0.0000988479
40.303781e6	0.000154123	0.0	0.000154123
50.007692e6	0.000761538	0.0	0.000761538
40.236090e6	0.002557559	0.195402	0.002557559
20.236090e6	0.005675431	0.596382	0.005675431
5.257557e6	0.011733119	0.894865	0.011733119
Concrete tension stiffening		Concrete tension damage	
Stress [Pa]	Cracking strain	Damage	Cracking strain
1.99893e6	0.0	0.0	0.0
2.842e6	0.00003333	0.0	0.00003333
1.86981e6	0.000160427	0.406411	0.000160427
0.862723e6	0.000279763	0.69638	0.000279763
0.226254e6	0.000684593	0.920389	0.000684593
0.056576e6	0.00108673	0.980093	0.00108673

associated with the failure mechanisms that occur in concrete. The plastic-damage model was originally developed by Lubliner *et al.* (1989) and Lee and Fenves (1998).

Modelling of the concrete-reinforcement interaction and energy release at cracking is of critical importance to the response of structure once the concrete starts to crack. These effects are modelled in an indirect way by adding “tension stiffening to the concrete model. The model parameters for the concrete structure are shown in Table 3 and obtained from Jankowiak and Lodygowski (2005) which gives definitions and derivations of all necessary parameters for a concrete grade of B50.

### 2.3.2 Steel reinforcement model

Steel reinforcement is modelled using the Rebar option. It can be defined as layers of uniformly spaced reinforcing bars in the host concrete solid elements. Such layers are treated as a smeared layer with a constant thickness equal to the area of each reinforcing bar divided by the reinforcing bar spacing. These layers have material properties that are different from those of the host element. The concrete behaviour is therefore considered as independent from that of the reinforcing bars. The effects associated with the rebar-concrete interface, such as bond slip and dowel action, are normally modelled approximately by introducing “tension stiffening into the concrete model to

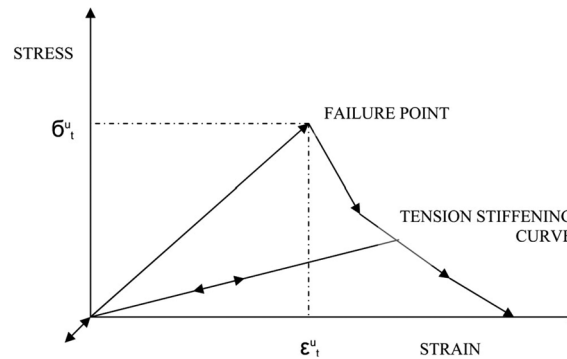


Fig. 1 Tension stiffening model

simulate the load transfer across cracks through the rebar. Tension stiffening is defined as plastic strain at which the cracking stresses causing tensile failure of the concrete reduce to zero. This reduction of tensile cracking stresses with plastic strain can be linear or multilinear. Reinforcement law is defined as multi-linear according to Fig. 1. Limited ductility can be also modeled by prescribing a limit strain. The smeared reinforcement is formulated as a material component of the composite material. The steel reinforcing bars are considered as elastic-perfectly plastic materials (i.e., without hardening) in both tension and compression. The model parameters used for this study are: density =  $7800 \text{ Kg/m}^3$ , Young's modulus ( $E$ ) =  $200 \text{ GP}$ , Poisson's ratio ( $\nu$ ) =  $0.3$  and the yield stress  $f_y = 220 \text{ MPa}$ .

#### 2.4 Soil-structure interaction

A precise simulation of the soil-structure interface is vital for a successful modelling of the system response. Preliminary studies have been undertaken to investigate the effect of interface characteristics on the response of concrete structures buried in soils with a range of properties subjected to dynamic impact load (Nagy 2007). The results showed clearly that the structure response is drastically affected by the characteristics of the soil-structure interaction. The friction along the interface directs how the loads and/or displacements are transferred from the surrounding soil to the structure. With the inclusion of a sliding interface the deformation of the buried structure was up to 5-folds that experienced for a fully joined structure with the surrounding soil. This indicates that in case of fully bonded mesh, only a small portion of the load would be transferred to the buried structure. These results are consistent with previous research studies (Yang 1997 and Weidlinger and Hinman 1988). Thus, a "finite sliding formulation is used which allows for any arbitrary motion of the surfaces such as separation, sliding, rebound and rotation of the surfaces in contact, which should be needed in the analysis of the structure response.

The classical theory of the Coulomb friction model is employed to relate the maximum allowable frictional (shear) stress across an interface to the contact pressure between the contacting surfaces. In the fundamental form of the Coulomb friction model, the two interacting surfaces can transmit shear stresses up to a certain limit through their interface before they start sliding relative to each other. This condition is known as sticking. The Coulomb friction model characterizes this critical shear stress,  $\tau_{cr}$ , at which sliding of the surfaces starts as a fraction of the contact pressure ( $P$ ) between the surfaces ( $\tau_{cr} = \mu P$  where  $\mu$  is the coefficient of friction (Nagy 2007). The interface

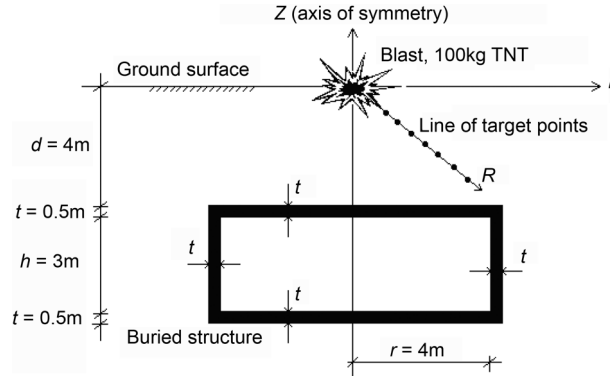


Fig. 2 Schematic diagram of the case study

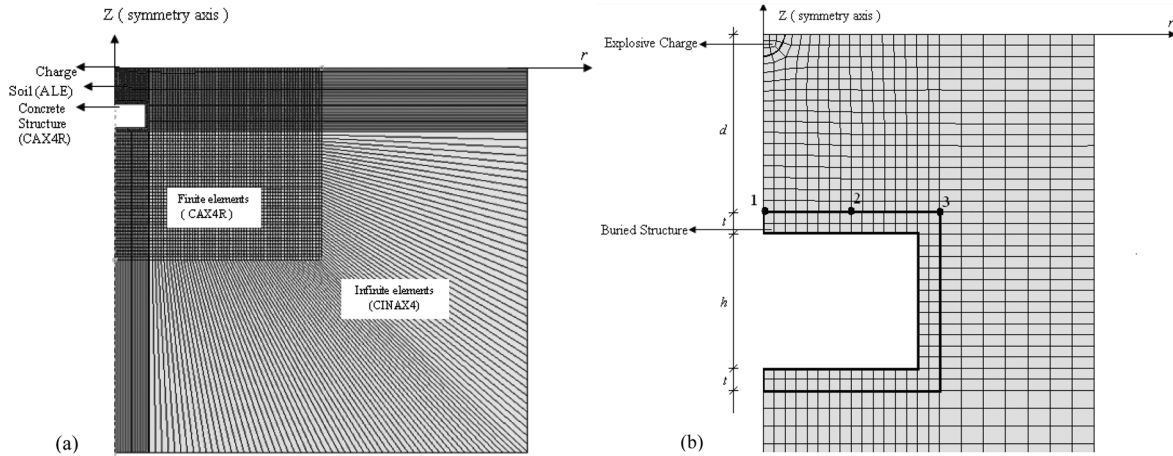


Fig. 3 The finite element mesh

characteristics between the soil and structure are investigated by considering the tangential behaviour with the coefficient of friction  $\mu=0.5$ .

### 3. Model discretisation with example application

When investigating the structure response for the purpose of designing the wall, the worst charge location is directly opposite to the centre of the wall. On the other hand if the purpose is to design the roof, the worst charge location is directly above the centre of the roof slab. Comparing the two cases considering the chosen structure dimensions shown in Fig. 2, it can be concluded that the worst case to be investigated is when the charge is directly above the roof slab centre point.

In this paper, the analysis procedure proposed above is used to undertake a two-dimensional (2D) axisymmetric analysis of the problem shown in Fig. 2. The ALE is used in the analysis to model both the charge region and the soil region close to the explosion. This is to eliminate the distortion of the mesh under high deformation (Hu and Randolph 1998). The overall geometric model is divided into three different regions representing the soil, structure and explosive materials. A convergence study involving mesh refinement, appropriate selection of element types and simulation

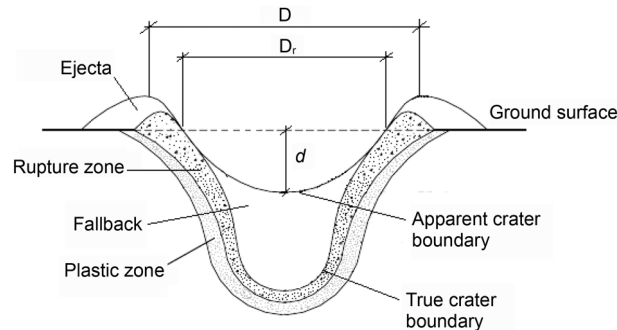


Fig. 4 Cross sectional dimensions of a typical crater

of the infinite boundaries was initially performed; hence the optimum meshes are identified for the soil, explosive charge (TNT) and the structure, as shown in Fig. 3. A TNT explosive charge is considered in this investigation with a mass of 100 kg.

The structure is modelled as a cylindrical reinforced concrete structure with constant thickness ( $t$ ) of 0.5 m through all its elements, internal height ( $h$ ) of 3.0 m and radius ( $r$ ) of 4.0 m. The structure is buried in the soil at a depth ( $d$ ) of 4.0 m below the ground surface. The structure is centred under the explosive charge as shown in Fig. 2.

The entire explosion-soil-structure system is represented by an assemblage of a finite number of 4-node bilinear axisymmetric quadrilateral, reduced integration elements (CAX4R). Smaller elements are used in the higher stress region and progressively larger elements in the lower stress region as shown in Fig. 3. Symmetry boundary conditions are applied along the axis of symmetry by restraining the displacement in the radial direction. Infinite elements (CINAX4) are used to provide quiet boundaries at the right side and bottom boundaries of the mesh as shown in Fig. 3(a). The infinite elements help to minimize any spurious wave reflections and thus simulate a boundary at infinity. The material models and parameters for the soil, concrete, reinforcing steel bars and TNT charge described in the previous sections are implemented in the model.

## 4. Results and discussion

Since the initial static stresses and pressures are all very small (0.04 MPa) in comparison with the anticipated stresses generated by the explosion, results are presented in terms of dynamic response only. As the proposed model provides a complete coupled analysis for the specified problem, the whole system behaviour including crater formation, blast wave propagation in soil, soil-structure interaction effects and the structure response are presented and discussed. In particular the response of the structure roof is considered as this is the most critical part of the structure from a design point of view.

### 4.1 Crater formation

Results of previous investigations indicated that a shallow explosion in soils produces a crater, while a deep explosion usually forms a cavity inside the soil and heave on the surface. Fig. 4 shows a schematic diagram of a cross sectional view of the crater demonstrating different zones and parameters,  $D$  is the apparent diameter of the crater,  $D_r$  is the true crater diameter and  $d$  is the

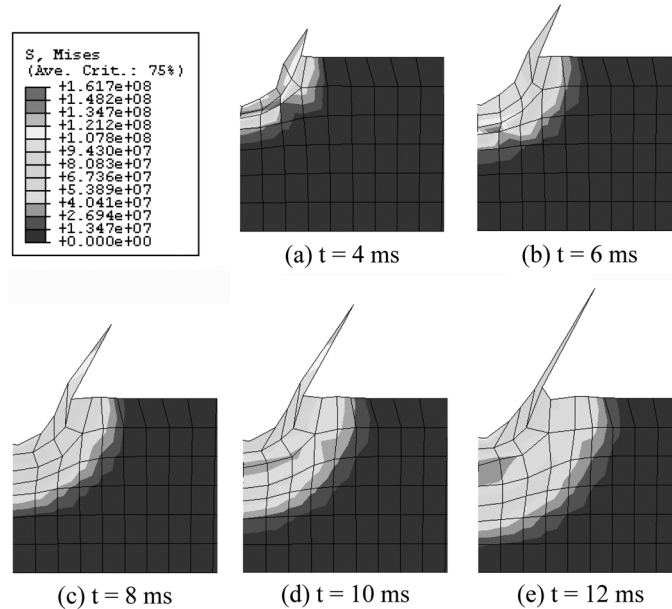


Fig. 5 Crater formation

apparent depth of the crater. The presented crater cross section shape is for an explosive charge positioned on or just below the ground level. The crater dimensions are based on the definitions of Kinney and Graham (1985) and Cooper (1997) which are used in this study.

Numerical formation of the whole crater for the 100 kg of TNT charge located on the soil surface in presence of the structure buried at 4 m depth is shown in Fig. 5 at times up to 12 ms after the explosion initiation. The figure also shows the Von Misses stresses developed in the soil and the crater progression from 4 ms to 12 ms. It can be seen that immediately after detonation the value of stress is high in the region close to the explosion-soil interface. With time, the stress wave propagates into the soil mass resulting in an attenuation of the stresses. This results in the formation of rupture and plastic zones as described in Fig. 4. Also shown in Fig. 5 is the ejecta whose height increases with time after explosion. The maximum height of the ejecta is reached at 12 ms after the explosion. The results of crater formation after 12 ms provide no additional information, which indicates that 12 ms is sufficient for the completion of crater formation. It is found that the formed crater from this explosion has a diameter of 2.28 m and a depth of 1.25 m.

As a verification of the finite element analysis, a comparison with experimental and numerical results is first carried out. The results of a series of tests performed by Ambrosini *et al.* (2002) with different amounts of explosive from 1 kg to 10 kg on the soil surface are used to calibrate the material and model parameters. The explosive charges used in these tests were Gelamon 80 a NG (Nitro Glycerine) based gelatinous explosive theoretically equivalent in mass to 80% of TNT. In order to perform a validation and comparative analysis the mass of explosive was defined by TNT equivalent mass. In order to get the corresponding mass for any other kinds of explosive, the concept of TNT equivalence stated by Formby and Wharton (1996) and Smith and Hetherington (1994) can be used. The numerical results performed by Nagy *et al.* (2007) with different amounts of explosive from 1 kg to 640 kg on the soil surface are used also to calibrate the material and model parameters. The previous numerical and experimental results were both obtained in a free-

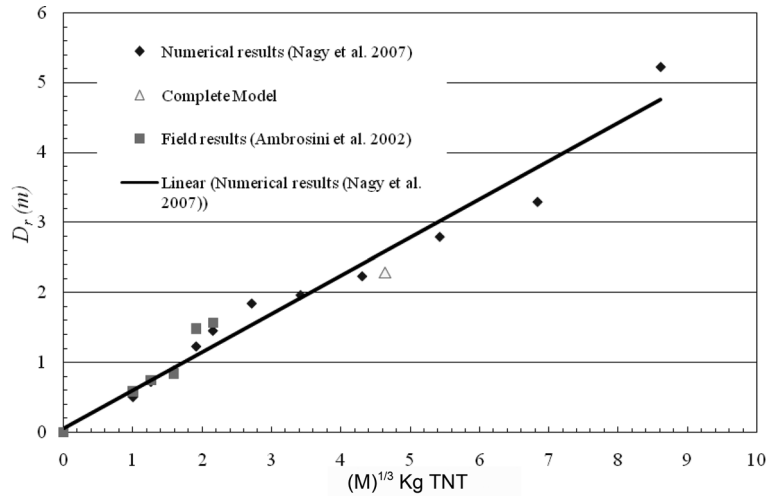


Fig. 6 Evaluation of crater diameter

field analysis (i.e., without the presence of a buried structure). In the current application analysis the concrete structure is buried at too deep a distance to affect the crater formation as the shock wave takes from 10 to 12 ms to reach the structure surface while the full crater formation is completed by 12 ms as discussed above.

Fig. 6 shows the obtained crater diameter by the proposed complete model compared with the results from the field test obtained by Ambrosini *et al.* (2004) and results of the numerical investigations obtained by Nagy *et al.* (2007). The comparison exercise demonstrates that there is a good agreement between the crater diameter obtained by the proposed complete model and those based on previous experimental and numerical investigations. Comparing to previous work it is therefore concluded that the new complete model is able to simulate correctly the crater formation resulting from the surface explosions.

#### 4.2 Blast wave propagation in the soil mass

To monitor the blast wave propagation in the soil mass, a group of target points is selected on a line inclined at 45° to the ground surface as shown on Fig. 2. The target points are located within the range  $R=0.9$  to 3.75 m (where  $R$  is measured from the centre of the explosion to the target point - see Fig. 2), located so as to be remote from the free surface and boundary condition effects.

The free field pressure can be obtained using the general empirical equation proposed in the design Manual (TM5-855-1 1986) for different kinds of soil. The empirical equation is based on a number of field tests and given as follows

$$PP = c \left( \frac{R}{M^{1/3}} \right)^{-n} \quad (2)$$

where the constant  $c$  is a typical value obtained from the TM 5-855-1 (1986) design Manual and depends on the charge material and soil properties. The constant  $n$  is the attenuation factor which depends mainly on the soil properties; (see for example, TM 5-855-1 1986 and Bulson 1997). Also in Eq. (2),  $R$  is the distance from the centre of the charge, and  $M$  is the mass of the charge. Table 4

Table 4 Constants of the free field pressure equation

	c	n
Upper empirical limit	1.12	2.75
Lower empirical limit	0.65	2.5
Numerical results	1.03	2.4797

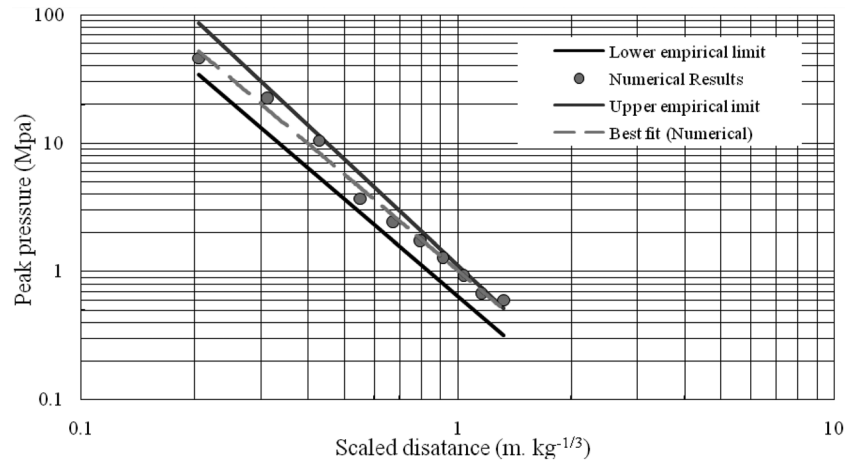


Fig. 7 Pressure attenuations with respect to the scaled distance

presents the constants  $c$  and  $n$  that are obtained from the design Manual for a clay soil with properties given in Table 1.

Fig. 7 shows a comparison between the numerically obtained results and the empirical peak total pressure attenuations plotted against the scaled distance ( $R/(\sqrt[3]{M})$ ). Since the soil properties in the TM 5-855-1 (1986) design Manual are provided for soil ranges according to soil types and are not closely defined in the numerical technique, Fig. 7 shows two straight lines representing the upper empirical limit and the lower empirical limit of the peak pressure in the considered soil type range. The empirical results represented by the two straight lines in Fig. 7 are based on the constant values presented in Table 4. The numerical results show that attenuation of the peak pressure in the soil occurs with increasing distance from the charge. It can be noted that the numerically obtained results of the peak pressure are in between and close to the upper and lower limits of the empirically obtained peak values for this kind of soil. The constants  $c$  and  $n$  in Eq. (2) are obtained using the best fit line for the numerical results. The constants obtained from the numerical results are also presented in Table 4. Inspection of the constants presented in Table 4 shows that both empirical equation and numerically developed equation have nearly the same attenuation factor  $n$  and a slight difference in the constant  $c$  but still within the range of the empirical values which mainly based on physical tests. Thus the results obtained are quite sensitive to relative variation in soil properties. The results obtained using the proposed analyses are therefore considered in good agreement with those derived from the physical testing.

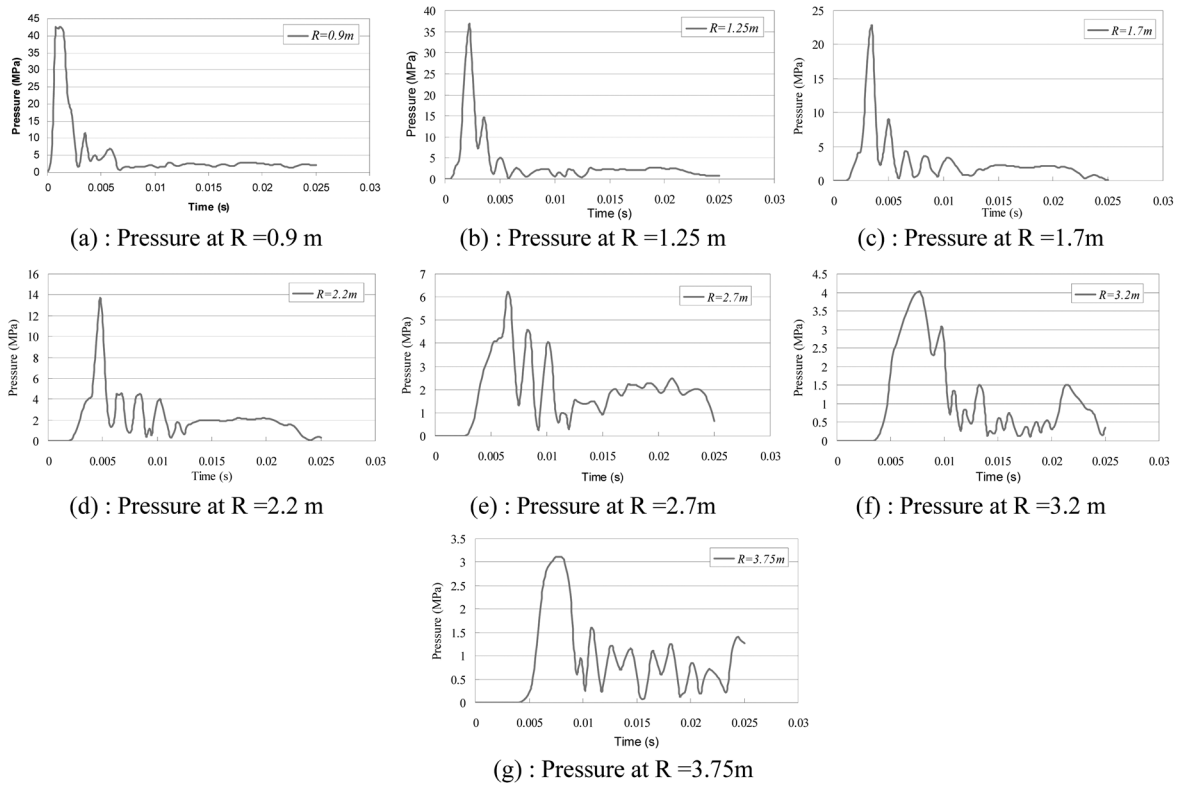


Fig. 8 Blast wave propagation through the soil mass

### 4.3 Blast wave propagation in the soil mass containing the buried structure

The overpressure histories are investigated at the same target points along the 45° inclined line from the charge centre to the structure. Figs. 8a to 8g show the numerical results of pressure against time after the explosion at particular locations. It can be seen that the attenuation of the peak pressure increases with increasing distance  $R$  from the centre of the explosion. It can also be noticed that three important conclusions can be obtained from these pressure histories;

- (i) The peak pressure attenuates rapidly with increase in distance from the centre of the explosion.
- (ii) The maximum value of the initial (incident) shock wave reduces with  $R$  (distance from the explosion) and occurs at a later time. At small values of  $R$  the dynamic response decays rapidly following the initial shock wave (see Fig. 8a), whereas as  $R$  increases this effect is less marked (see Fig. 8g). Fig. 9 shows all these features superimposed.
- (iii) For the target points closer to the buried structure, the reflected waves are larger in proportion to the incident wave, an effect that was also observed by Leppanen and Gyloft (2003). Indeed over the period considered all target points appear to have reached an approximately equal steady state dynamic response after the initial rapid decay. This is due to increasing interaction between the soil and structure as the structure is approached, and a lower level of damping in the structure than in the soil.

These results clearly show that the proposed complete numerical coupled model can represent the

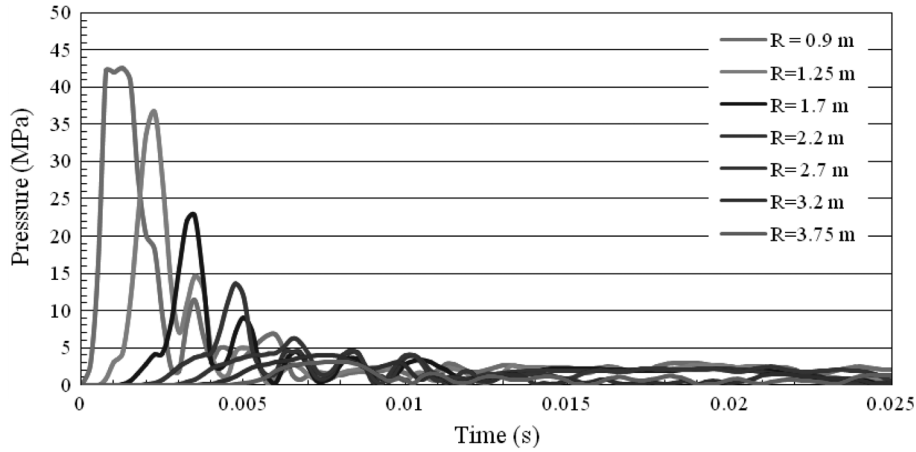


Fig. 9 Pressure at target points along 45° inclined line from the charge centre

behaviour of non-linear soil-structure systems under blast loads in a realistic way. In particular the analysis automatically provides a means to analyse the blast wave propagation through the soil and the deformation mechanism of the soil under rapidly decaying explosion loads.

#### 4.4 Structure response

##### 4.4.1 The roof slab behaviour

As the roof slab is the most critical element of the structure in this problem, a number of target points on the roof are selected to record the structure response. These points are; the roof centre point (1), the quarter span roof point (2) and the corner roof point (3). These points are highlighted in Fig. 3b.

Figs. 10 and 11 present the results of vertical and lateral displacement time histories on the roof slab respectively. The results are presented for the target points 1, 2 and 3. It can be seen that noticeable permanent displacements of the roof structure slab occur in both the vertical direction (with a range of 2~15 mm) and lateral direction (with a range of 3~10 mm). The difference in the behaviour of the concrete slab at these three points is due to the variation of the pressure generated

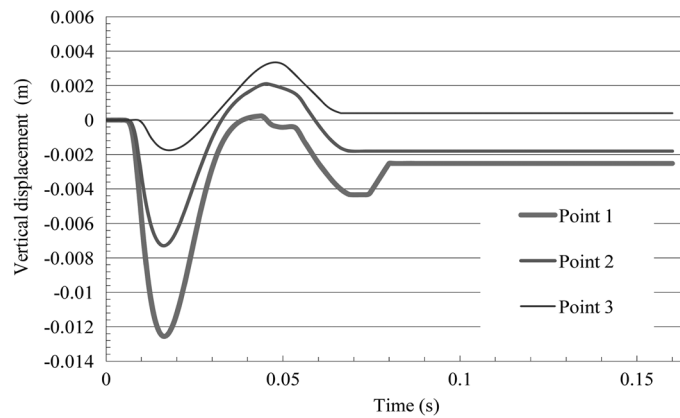


Fig. 10 Vertical displacement of the roof slab

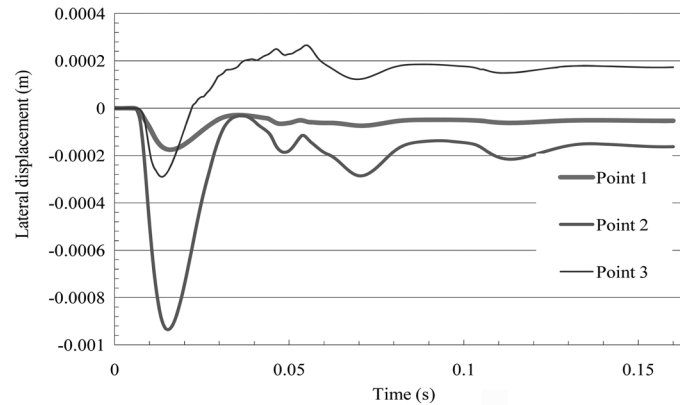


Fig. 11 Lateral displacement of the roof slab

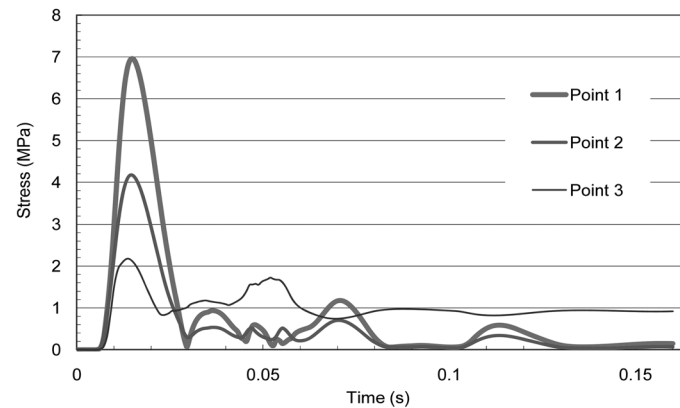


Fig. 12 Stresses at target points on the structure roof

by the explosion loads as well as due to the nonlinearity of the concrete and reinforcement models. The residual deflections indicate the occurrence of plastic deformation.

Fig. 12 shows the blast overpressure on the roof slab of the structure at a number of target points to capture the structure response. As anticipated from the deflection results, the contact stresses differ considerably between the target points. After the initial shock pulse a longer period of oscillations occurs, indicating the involvement of the structural response. The peak overpressure tends to decrease progressively with distance from the roof centre point. The peak pressure near the corner target point 3 is only 30% of that at the centre point 1.

In addition Fig. 12 shows that following the incident wave the contact pressure between structure and soil is significantly higher at target point 3 than at target points 1 and 2. Thus the structure has suffered permanent deformation at points 1 and 2, and an arching effect has developed in the soil to relieve the load on the deflected structure. This behaviour has also been observed by Chen *et al.* (1990) which provides further supporting evidence of the validity of the soil structure interaction modelling incorporated in this analysis.

#### 4.4.2 Structure damage evaluation

Fig. 13 shows the damage suffered by the concrete structure. Results from the concrete damage

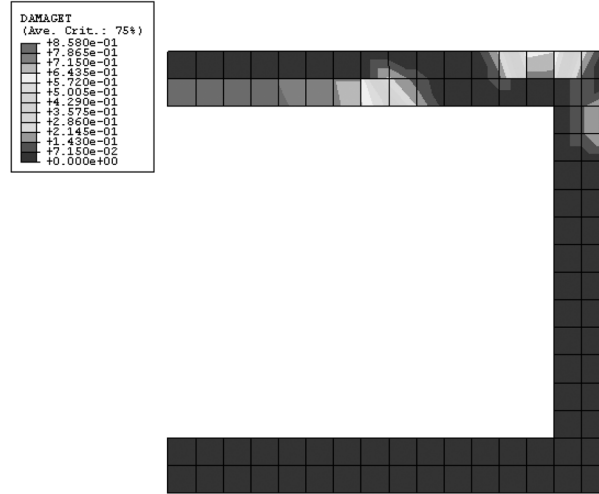


Fig. 13 Damage in concrete structure

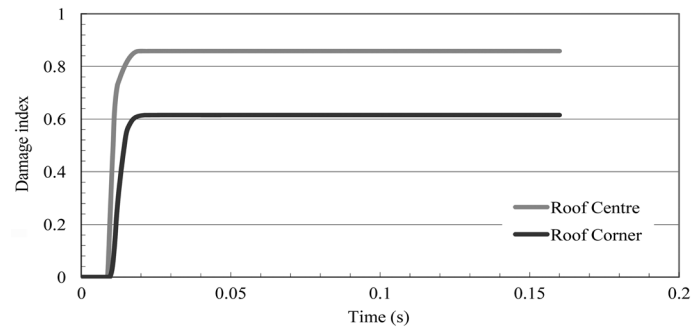


Fig. 14 Damage index of the structure roof

plasticity model indicate that the damage occurs primarily at the centre of the roof slab. The remaining parts of the buried structure show more or less a uniform distribution of little damage. As would be intuitively expected, damage occurred at the centre of the roof due the high level of exposure there to the explosion shock wave as can be seen from Fig. 13.

Fig. 14 shows that the maximum values of the damage indexes for both the centre and the corner of the roof slab to be close to 0.85 and 0.61 respectively. The degree of damage in the rest of the buried structure is generally minor with a damage index below 0.2. This may be explained by the fact that the elements not subjected to the direct shock suffer reduced loading in a manner directly analogous to the equivalent static problem. Since a damage index of 0.7 indicates severe damage and beginning of failure (Kim *et al.* 2005) this analysis implies that the roof to this structure needs to be strengthened if all other parameters remain unchanged.

## 5. Conclusions

- A complete coupled numerical model to simulate the behaviour of a reinforced concrete buried structure under the effect of blast loads has been developed and presented in this paper. The

analysis models the explosion process of the charge, the propagation of stress waves through the soil medium, the interaction of the buried reinforced concrete structure with the surrounding soil and the structure response in one single stage and therefore represents a definite improvement on previous simulations.

- The results obtained for the example problem indicate that there is a good agreement between crater diameter and that obtained by previous experimental and numerical investigations. The results also highlight the significance of the first peak of the structural response to the explosion load. In addition the adopted model for the interface effects between soil and structure including the slip action has been successful. Nevertheless, there remains a need for good quality comparative physical test data in order to fully verify the results obtained from numerical modelling.
- The complete model provides with an improved computational tool for the design of buried concrete structures. Through FEA modelling, the damage failure mode and the damage failure locations can now be determined. In addition the extent of the strength and serviceability improvements that can be achieved by appropriate redesign of the system can be identified.

## References

- ABAQUS Analysis Manual, Version 6.5. (2005), Published by Hibbitt, Karlsson And Sorensen Inc. USA.
- ABAQUS Theory Manual, Version 6.5. (2005), Published by Hibbitt, Karlsson And Sorensen Inc. USA.
- Ambrosini, R.D., Luccioni, B.M., Danesi, R.F., Riera, J.D. and Rocha, M.M. (2002), "Size of craters produced by explosive charges on or above the ground surface", *Shock Waves*, **12**, 69-78.
- Ambrosini, D., Luccioni, B. and Danesi, R. (2004), "Influence of the soil properties on craters produced by explosions on the soil surface", *Mechanica Computacional*, XXIII.
- Baylot, J.T. (1992), "Parameters affecting loads on buried structures subjected to localized blast effects", *U.S.A.E.W.E.S. Technical report SL-92-9*, Vicksburg, Miss., US.
- Bulson, P.S. (1997), *Explosive Loading of Engineering Structures*, Spon Press, London.
- Casadei, F., Halleux, J.P., Sala, A. and Chille, F. (2001), "Transient fluid-structure interaction algorithms for large industrial applications", *Comput. Method. Appl. M.*, **190**(24-25), 3081-3110.
- Chen, H.L., Shah, S.P. and Keer, L.M. (1990), "Dynamic response of shallow buried cylindrical structures", *J. Eng. Mech.*, **116**(1), 152-171.
- Chen, W.F. and Mizuno, E. (1990), *Nonlinear analysis in soil mechanics theory and implementation*, Elsevier Science Publishers, B.V. 672.
- Drucker, D.C. and Prager, W. (1952), "Soil mechanics and plastic analysis or limit design", *Q. Appl. Math.*, **10**, 157-165.
- Formby, S. and Wharton, R.K. (1996), "Blast characteristics and TNT equivalence values for some commercial explosives detonated at ground level", *J. Hazard. Mater.*, **50**(2-3), 183-198.
- Helwany, S. (2007), *Applied soil mechanics with ABAQUS' applications*, Hoboken, New Jersey, John Wiley & Sons, Inc.
- Henrych, J. (1979), *The dynamics of explosion and its use*, New York, USA, Elsevier.
- Hinman, E.E. (1989a), "Effect of deformation on the shock response of buried structures subject to explosions", *Structures under shock and impact*, Elsevier, 455-465.
- Hinman, E.E. (1989b), "Shock Response Of Buried Structures Subject To Blast", *Structures For Enhanced Safety And Physical Security*, Amer. Soc. Civil Engineers, New York, 191-202.
- Hu, Y. and Randolph, M.F. (1998), "A practical numerical approach for large deformation problems in soil", *Int. J. Numer. Anal. Meth. Geomech.*, **22**(5), 327-350.
- Jankowiak, T. and Łodygowski, T. (2005), "Identification of parameters of concrete damage plasticity constitutive mode", *Found. Civil Environ. Eng.*, **6**, 53-69.
- Kanarachos, A. and Provatidis, C.H. (1998), "Determination of buried structure loads due to blast explosions", *Structures under Shock and Impact*, 95-104.

- Kim, T.H., Lee, K.M., Chung, K.M. and Shin, H.M. (2005), "Seismic damage assessment of reinforced concrete bridge columns", *Eng. Struct.*, **27**(4), 576.
- Kinney, G.F. and Graham, K.J. (1985), *Explosive shocks in air*, 2<sup>nd</sup> Edition, New York, Springer Verlag.
- Lee, E.L., Hornig, H.C. and Kury, J.W. (1968), *Adiabatic expansion of high explosive detonation products*, Lawrence Radiation Laboratory, University of California, UCRL-50422.
- Lee, E., Finger, M. and Collins, W. (1973), *JWL equations of state coefficient for high explosives*, Lawrence Livermore Laboratory, Livermore, Calif, UCID-16189.
- Leppänen, J. and Gylltoft, K. (2003), "Concrete Structures Subjected to Blast and Fragment Impacts", *J. Nordic Concrete Res.*, **29**, 65-84.
- Lee, J. and Fenves, G.L. (1998), "Plastic-damage model for cyclic loading of concrete structures", *J. Eng. Mech.*, **124**(8), 892-900.
- Lu, Y. and Wang, Z. (2006), "Characterization of structural effects from above-ground explosion using coupled numerical simulation", *Comput. Struct.*, **84**(28), 1729.
- Lu, Y., Wang, Z. and Chong, K. (2005), "A comparative study of buried structure in soil subjected to blast load using 2D and 3D numerical simulations", *Soil Dyn. Earthq. Eng.*, **25**(4), 275-288.
- Lubliner, J., Oliver, J., Oller, S. and Oñate, E. (1989), "A plastic-damage model for concrete", *Int. J. Solids Struct.*, **25**(3), 229-326.
- MIL-HDBK-1007/3, (1997), *Soil dynamics and special design aspects*, Department of Defence, US Army NFESC.
- Mueller, C.M. (1986), *Shear friction test support programme; laboratory friction test results for WES flume sand against steel and grout*, Report 3, USAE WES, Technical report SL-86-20, Vicksburg, Miss.
- Nagy, N. (2007), *Dynamic soil structure interaction of buried concrete structures under the effect of blast loads*, PhD thesis, University of Bradford.
- Nagy, N., Mohamed, M. and Boot, J. (2007), "Numerical investigation of surface explosion effects on clay soils", *Proceedings of the 4<sup>th</sup> International Conference on Earthquake Geotechnical Engineering*. Thessaloniki, Greece.
- O'Daniel, J.L. and Krauthammer, T. (1997), "Assessment of numerical simulation capabilities for medium-structure interaction systems under explosive loads", *Comput. Struct.*, **63**(5), 875-887.
- Smith, P.D. and Hetherington, J.G. (1994), *Blast and ballistic loading of structures*, Butterworth and Heinemann Ltd Oxford.
- Stevens, D.J. and Krauthammer, T. (1988), "A finite difference / finite element approach to dynamic soil structure interaction modeling", *Comput. Struct.*, **29**(2), 199-205.
- Stevens, D.J., Krauthammer, T. and Chandra, D. (1991), "Analysis of blast-loaded, buried arch response", *Part II: Application, J. Struct. Eng. - ASCE*, **117**(1), 213-234.
- TM 5-855-1 (1986), *Fundamental of protective design for conventional weapons*, Vicksburg, US, US Army Engineers Waterways Experimental Station.
- Wang, Z.Q., Lu, Y., Hao, H. and Chong, K. (2005), "A full coupled numerical analysis approach for buried structures subjected to subsurface blast", *Comput. Struct.*, **83**(4-5), 339-356.
- Wang, Z., Hao, H. and Lu, Y. (2004), "A three-phase soil model for simulating stress wave propagation due to blast loading", *Int. J. Numer. Anal. Met. Geomech.*, **28**(1), 33-56.
- Weidlinger, P. and Hinman, E. (1988), "Analysis of underground protective structures", *J. Struct. Eng.*, **114**(7), 1658-1673.
- Zhang, Y.D., Fang, Q. and Liu, J.C. (2002), "Experimental and numerical investigations into responses of buried RC frames subjected to impulsive loading", *Structures under shock and impact VII*, Elsevier, 69-78.
- Zimmerman, H., Cooper, G., Carney, J. and Ito, Y. (1990a), *Cratering and ground shock environment prediction of buried armor piercing bomb in dry Socorro plaster sand*, Technical Report CRT-3295-010-01, California Research and Technology, Chatsworth Calif.
- Zimmerman, H., Cooper, G., Carney, J. and Ito, Y. (1990b), *Cratering and ground shock environment prediction of buried armor piercing bomb in 3% AFV fort knox clay backfill*, Technical Report CRT-3295-010-02, California Research and Technology, Chatsworth Calif.
- Yang, Z. (1997), "Finite element simulation of response of buried shelters to blast loadings", *Finite Elem. Anal. Des.*, **24**, 113.